Research Square

Preprints are preliminary reports that have not undergone peer review.
They should not be considered conclusive, used to inform clinical practice,
or referenced by the media as validated information.

Restoring myelination in rat sciatic nerve using BM-MSCs and conditioned media

Aparna Mohanty
L V Prasad Eye Institute
Aluru Venkata Saijyothi
University of Hyderabad
Megha Shantveer Uppin
Nizam's Institute of Medical Sciences
Geeta K Vemuganti
geeta.vemuganti@lvpei.org

L V Prasad Eye Institute

Article

Keywords: Demyelination, Partial Sciatic nerve Ligation, Remyelination, BM-MSCs, Conditioned media

Posted Date: July 23rd, 2026

DOI: https://doi.org/10.21203/rs.3.rs-10151893/v1

License: This work is licensed under a Creative Commons Attribution 4.0 International License.
Read Full License

Additional Declarations: No competing interests reported.

Restoring myelination in rat sciatic nerve using BM-MSCs and conditioned media

Aparna Mohanty [1], Aluru Venkata Saijyothi[2], Megha Shantveer Uppin [3], Geeta Vemuganti [*1]

[1] Centre for Ocular Regeneration, Prof. Brien Holden Eye Research Centre, Champalimaud Translational Centre for Eye research, L.V. Prasad Eye Institute, Hyderabad, India

[2] School of Medical Sciences; University of Hyderabad, Prof C R Rao Road, Gachibowli, Hyderabad, Telangana, India

[3] Department of Pathology; Nizam institute of Medical Sciences, Hyderabad, Telangana, India

*Corresponding author:

Dr. Geeta K Vemuganti

Distinguished Pathologist and Scientist,

L V Prasad Eye Institute

Kallam Anji Reddy Campus, L V Prasad Marg

Banjara Hills, Hyderabad 500034, India

Mail-id: geeta.vemuganti@lvpei.org, gkvemuganti@gmail.com

Phone: +91 40 2354 2617

Abstract

Damaged peripheral nerves post injury, causes loss of outer protective covering (demyelination) on the nerves resulting in loss of proper functioning. This becomes challenging due its progressive nature, limited satisfactory treatment, high morbidity, delayed diagnosis and prognosis. Exploring novel methods of treatment such as cell-based regeneration using stem cells seems promising. In this study, we have attempted to use stem cell therapy using cells (BM-MSCs) and the conditioned media (CM) to restore the nerve damage and myelination in the surgically induced rat injury model. Male Sprague Dawley (SD) rats (N=30) were divided into five groups: Control, nerve injury group, self-recovery, treatment group using cells and the conditioned media. Injury in the sciatic nerve was surgically induced by partial Sciatic nerve Ligation (PSNL). Post injury, the nerve revealed fibre loss, thinning of myelin sheath (demyelination) and axonal shrinkage as compared to control validated by histopathology and transmission electron microscopy (TEM). Treatment with BM-MSCs and CM reversed the nerve damage. The nerve looked structurally better with increased myelin thickness, axonal radius and healthier cells in comparison with injured nerve. Together our data reported that both BM-MSCs and CM can repair nerve damage and restore myelination, however cell-based therapy was better than CM. This study provides a preclinical evidence of treating nerve injuries and enhancing nerve regeneration in future.

Keywords - Demyelination, Partial Sciatic nerve Ligation, Remyelination, BM-MSCs, Conditioned media

Introduction

Injury to the peripheral nerves affects the myelin causing demyelination leading to secondary nerve injury, the extent of which decides the treatment modalities. Patients with mild peripheral nerve injuries might recover, while patients with severe peripheral nerve injuries (PNI) and long nerve defects often suffer from impaired motor, sensory and autonomic nerve functions and are in need of peripheral nerve repair surgeries[1]. Although capable of spontaneous regeneration, complete functional restoration in the peripheral nerves remains a concern for both researchers and clinicians. Specifically, therapeutic intervention or some form of tissue/cell-based therapy remains inevitable option for recovery from large PNI gaps. Autologous nerve grafting, considered the "gold standard" is regularly employed for treating of gap formation type PNI[2]. Other approaches include: cell based i.e. direct cell transplantation at the injury site, and cell free approach via delivery of growth factors for stimulating the nerves[3]. However, the use of SCs in clinical cell-based therapy is limited due to its less availability in sufficient quantity costing a healthy functional nerve from the donor, prolonged culture, expansion period in vitro and incomplete functional recovery [3-5]. This urged researchers and clinicians exploring alternative cells for transplantation purpose.

Bone marrow mesenchymal stem cells (BM-MSCs) are self-renewing, multipotent progenitors isolated from bone marrow that have the capability to promote tissue-repair and regeneration both in their native form and transdifferentiated form[6-8]. Since the recent reports suggest the benefit of BM-MSCs through a paracrine effect[9-11], we aim to explore the therapeutic potential of BM-MSCs and the conditioned media in restoring myelination in demyelinated rat model. The secondary outcome of this study is to evaluate the secretome of the conditioned media so as to understand the factors that could potentially serve as regenerative factors.

Results

Post surgery, the animals showed evidence of limping in all the groups. The animals in DEM group were sacrificed on day 21 and evaluated for evidence of demyelination.

Evidence for Demyelination

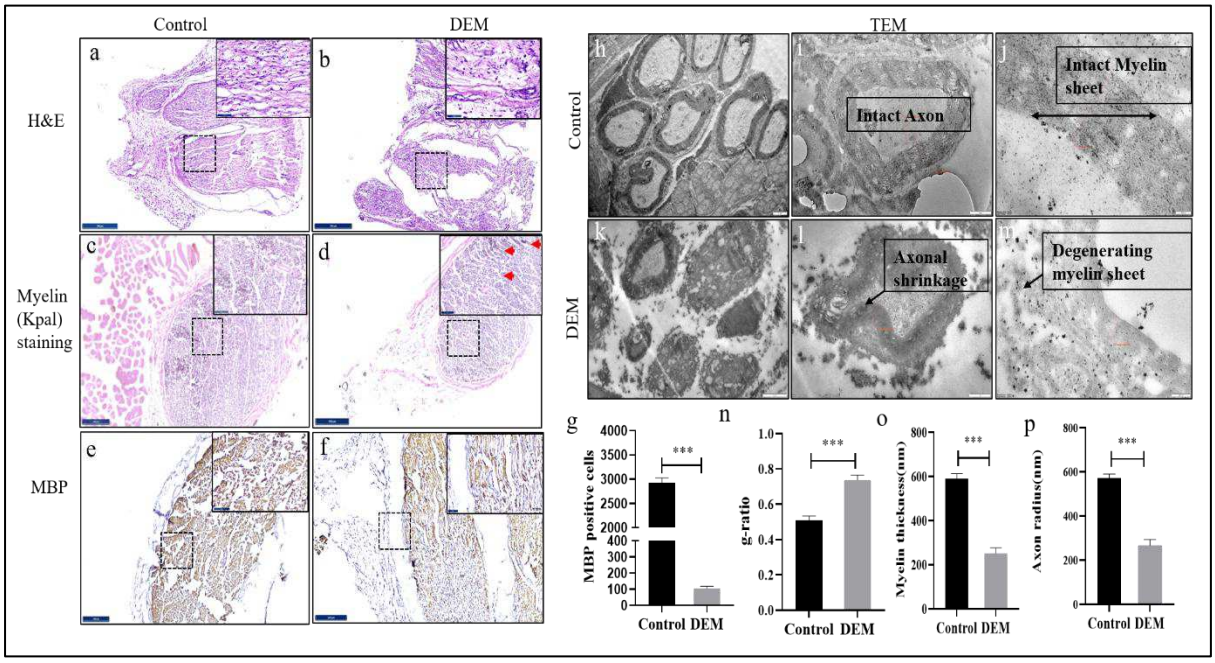


Fig.1 Histological and morphometric validation of surgically induced demyelination in sciatic nerve. Representative images of sections of sciatic nerve processed for H&E staining in different groups. a) Control b) DEM. Representative images of Myelin (Kpal) stain on sciatic nerve sections of various groups c) Control d) DEM. Immunohistochemistry (IHC) images for myelin basic protein (MBP) e) Control f) (DEM) g) Semi quantitative analysis of IHC showing MBP positive cells in different groups. Representative images of ultrastructural examination of sciatic nerve sections in different groups h, i, j) Control k, l, m (DEM). Quantification of various parameters from morphometric analysis of sciatic nerve sections in different groups n) g ratio (p***<0.01) Control vs DEM o) myelin thickness. (p****<0.0001) Control vs DEM p) axon radius. (p***<0.001) Control vs DEM. Scale bar for TEM micrographs h, i, k) 1µm, l) 500nm j, m)200nm. Scale bar 500µm and insert scale bar 20µm for H&E images. Scale bar 200µm and insert scale bar 20µm for myelin staining and IHC images. Data reported as mean ± standard deviation. p***<0.001 compared to control for IHC quantification).

Histopathology revealed intact nerve fibers in control group (Fig.1a), as compared to DEM group with overall architecture relatively disoriented, irregularly arranged nerve fibers, marked by disappearance of some nerve fibers (Fig.1b). Mylein staining (Kpal) staining revealed thin myelin rings in the DEM group indicating

demyelination/remyelination around the axons (Fig.1d) in contrast to the control group displaying optimal staining for Kpal with intense myelin rings (Fig.1c).

Additionally, immunostaining for myelin basic protein (MBP) revealed optimal expression of MBP in control groups (Fig.1e) as compared to DEM group (Fig.1f). Semiquantitative analysis for MBP expression further confirmed significant decrease in the MBP positive cells in DEM group as compared to control (Fig.1g).

Ultrastructural and morphometric analysis displayed intact axon and organized myelin sheath in the control (Fig.1h, i, j) whereas DEM group displayed distorted axonal morphology, interaxonal gaps, axonal shrinkage and disintegrated myelin sheath (Fig.1l, m). Analysis of morphometric parameters revealed significant difference in g ratio, myelin and axonal radius amongst control and DEM group (Fig.1n, o, p).

Evidence of Remyelination after Intravenous administration of BM-MSCs and the Conditioned Media

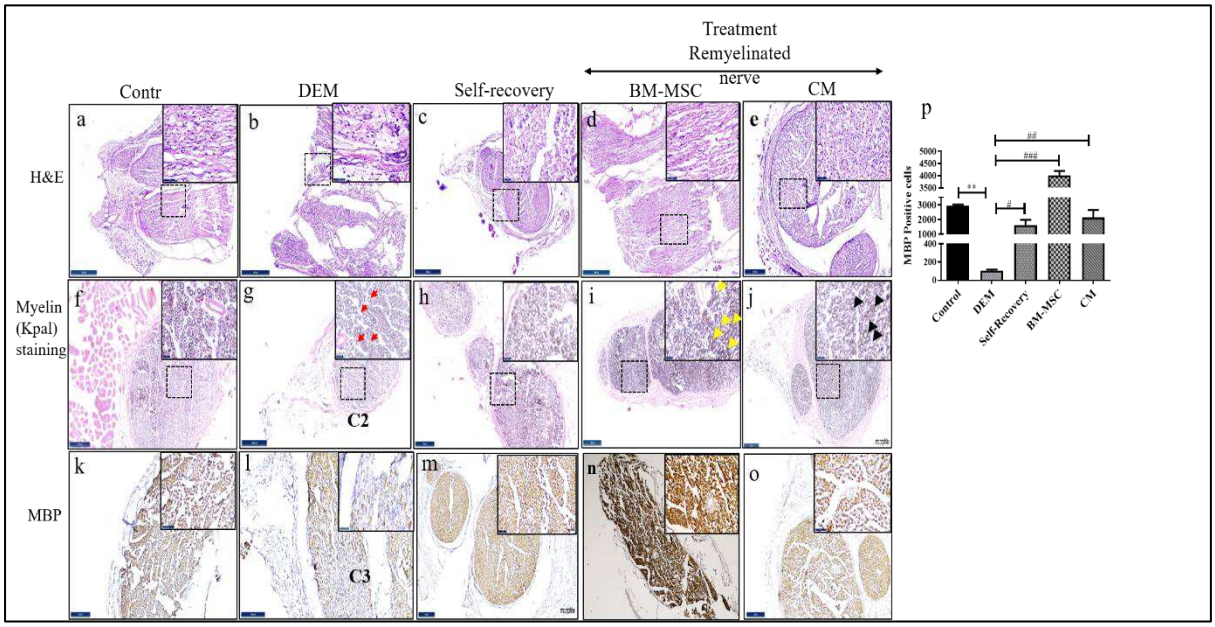


Fig.2 Histological and morphometric evaluation of remyelination post interventions. Representative images of sections of sciatic nerve processed for H&E staining in different groups. a) Control b) DEM c) Self-recovery d) BM-MSC e) CM. Myelin (Kpal) stain on sciatic nerve sections of various groups f) Control g) DEM h) Self-recovery i) BM-MSC j) CM. Immunohistochemistry (IHC) images for myelin basic protein (MBP) k) Control l) DEM m) Self-recovery n) BM-MSC o) CM p) Semi quantitative analysis of IHC showing MBP positive cells in different groups. Image scale bar 500µm and insert scale bar 20µm for H&E images. Image scale bar 200µm and insert scale bar 20µm for myelin staining and IHC images. Data reported as mean ± standard deviation. p***<0.001 compared to control, p#<0.01, p##<0.001 and p###<0.001 compared to demyelinated (DEM) group.

Histopathology revealed densely arranged tissues in control (Fig.2a) as compared to DEM group displaying disorderly arranged nerve fibers marked by disappearance of some nerve fibers (Fig.2b). In the immediate sciatic nerve repair group, tissue fibers proliferation and recovery were observed in both BM-MSCs (Fig.2d) and CM treated group (Fig.2e).

Myelination

Kpal staining for myelin displayed densely populated myelin rings around axons in control (Fig.2f) as opposed to DEM group displaying reduced myelin staining along with thin myelin rings denoted by red arrows demonstrating de/remyelination in the DEM (Fig.2g). No significant difference was observed in self-recovery group (Fig.2h) as compared to DEM. BM-MSCs and CM treated group displayed intense staining of dense myelin rings around axons suggesting remyelination. However, remyelination was better with BM-MSCs (Fig.2i) than CM (Fig.2j).

Re-expression of MBP

Immunostaining for MBP revealed presence of bulbous distorted myelin along with fiber loss in the tissue sections in the DEM group (Fig.2l) with optimal expression of the myelin protein with intact fibers observed in the control (Fig.2k). Post intervention, increase in MBP expression was observed in both BM-MSC and CM (Fig.2n, o) treated group suggesting myelin restoration, however expression was heightened with BM-MSCs as compared to CM. Semiquantitative analysis for MBP expression revealed increased (~ 95%) MBP expression in BM-MSC and (~ 52%) CM treated group respectively as compared to DEM group (Fig.2p).

Ultrastructural and morphometric evaluation of the nerve post intervention

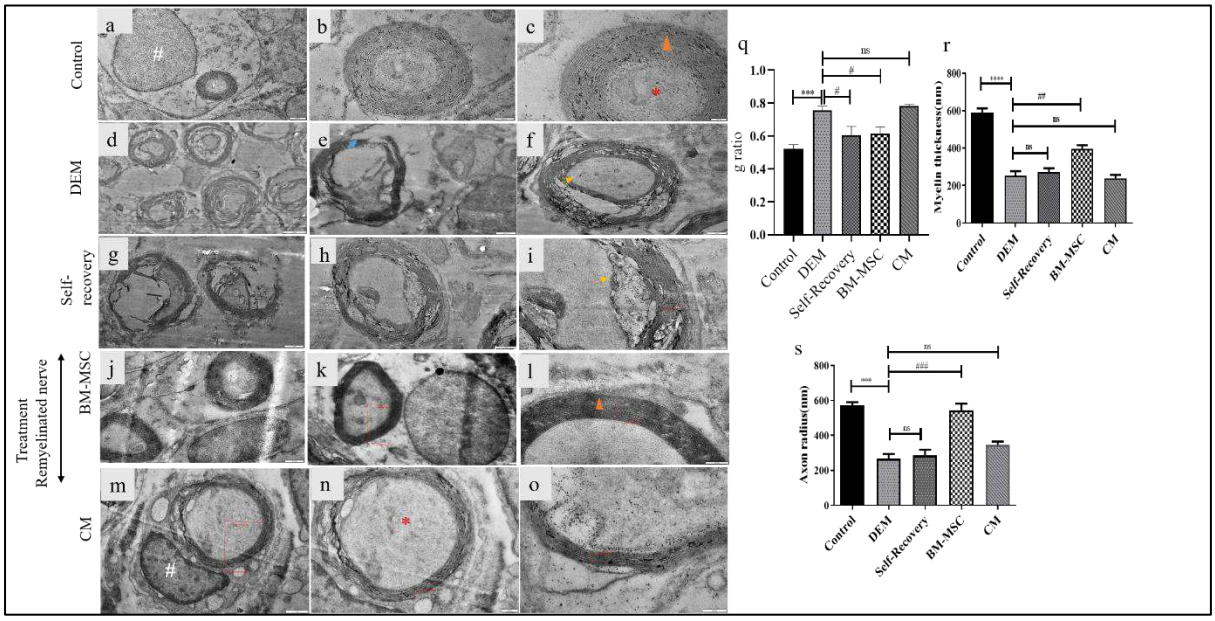


Fig.3 Representative images of ultrastructural examination of sciatic nerve sections in different groups. a, b, c) control d, e, f) DEM g, h, i) self-recovery j, k, l) BM-MSC m, n, o) Cells. # represents schwann cell nucleus, blue arrow represents degenerating myelin, orange triangle represents intact myelin, red star represents intact axon, yellow arrow represents inter axonal gap and axonal shrinkage. Scale bar a, d, g, h, m) 500nm, b, e, h, k, n) 1µm, c, f, i, l, o) 200nm. Quantification of various parameters from morphometric analysis of sciatic nerve sections in different groups q) g ratio (p***<0.01) Control vs DEM, (P #<0.01) DEM vs CM, ns=non-significant (p=0.9683) DEM vs CM r) Quantification myelin thickness. (p****<0.0001) Control vs DEM, (p ## <0.001) DEM vs BM-MSCs, ns=non-significant (p=0.9936) DEM vs CM s) axon radius. (p***<0.001) Control vs DEM, (p ###<0.001) DEM vs BM-MSCs, ns=non-significant (p=0.3718) DEM vs CM.

TEM images revealed disrupted myelin, axonal shrinkage and interaxonal gaps in DEM (Fig.3d, e, f) as compared to control (Fig.3a, b, c). Interestingly, increased myelin thickness, decreased interaxonal gap and ameliorated axonal shrinkage was observed in BM-MSC (Fig.3k, l) and CM group but lesser effect in CM (Fig.3n, o). Morphometric analysis displayed intact axon, increased myelin thickness (~57%), increased axonal radius (~96%) in BM-MSC treated group while CM group revealed increased myelin thickness (~ 5%) and axonal radius (~28%) as compared to DEM group suggesting remyelination.

Characterization of the CM harvested from BM-MSCs

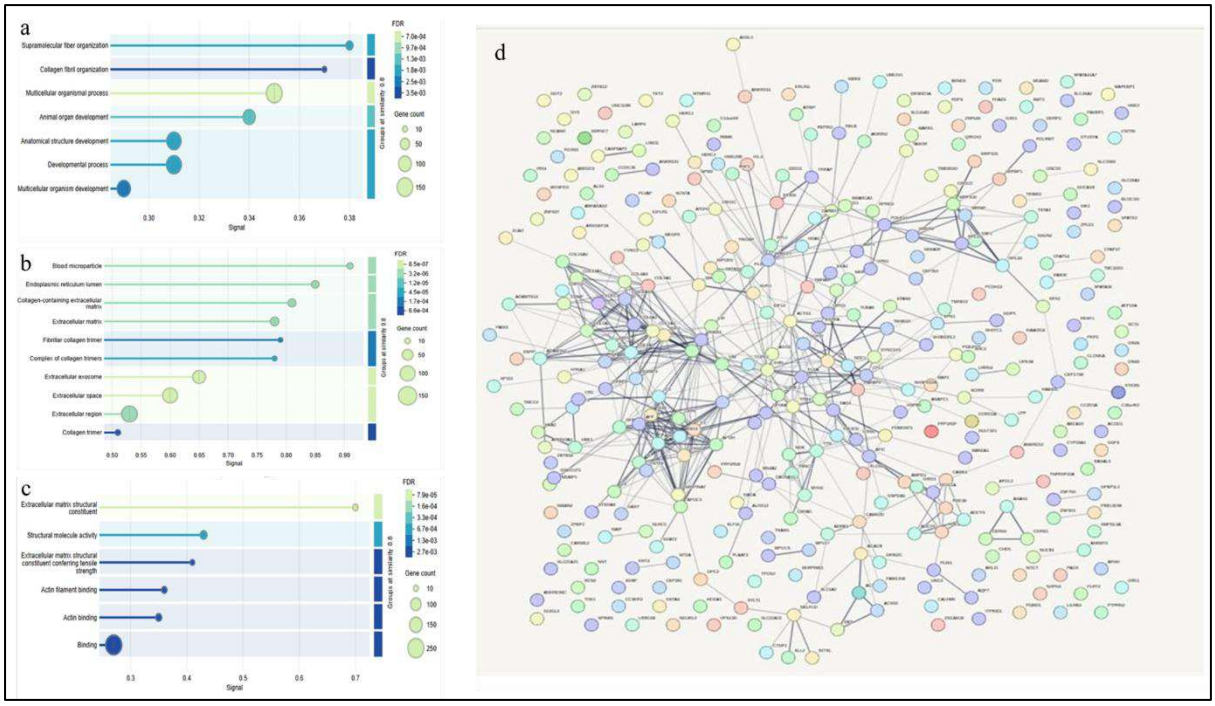


Fig.4 Characterization of secretome by mass spectrometry a) Biological process of BMSC secretome proteins. b) Molecular Function of BMSC secretome proteins c) Cellular proteins of BMSC secretome proteins. The proteins were categorized based on their False discovery rate (FDR) ≤ 0.05 when compared with the whole gene count. X-axis indicates the signal /gene count and the Y-axis indicates the Groups at similarity was set at 0.8.d) Representative image of the interacting proteins in BM-MSC secretome. A typical BM-MSC secretome protein association network using STRING. The network has been expanded by 346 valid proteins and the confidence cutoff for showing interaction links has been set to "highest" (0.900). The secretome proteins identified showed as various colored nodes. Each node represents all the proteins produced by a single protein-coded gene locus. The interaction of protein with other showed with edges. The line thickness indicates the strength of data support. The interactions of each protein are specific[12-14].

Among 515 proteins identified from mass spectrometric analysis, 346 proteins were identified as valid proteins for the analysis based on functional analysis. The functional annotations like involvement in biological process, presence in cellular components, and its molecular function was observed using STRING. The proteins were involved in various biological processes like supra molecular fiber organization, collagen fibril organization, animal organ development, developmental process, multicellular organ development etc. (Fig.4a) with more proteins in multicellular organismal process. The molecular function of the identified proteins has role in extracellular matrix structure, structural molecule activity, actin and actin filament binding and other binding

proteins (Fig.4b) with more proteins in binding molecular function. The cellular components of the secretome present in endoplasmic reticulum, extracellular matrix, fibrillary collagen trimers, extracellular region etc. with more proteins in extracellular region (Fig.4c). STRING analysis revealed large number of proteins interactions forming networks (Fig.4d). DAVID annotation KEGG pathway revealed the involvement of neurotrophic proteins, cholinergic proteins and proteins involved in neurodegenerative disease pathway, cellular differentiation, developmental process and vesicle trafficking listed in Table 2. Some of the below mentioned proteins were found to be involved in neurological pathway.

Table 2: KEGG pathway analysis of BM-MSC secretome proteins involved in neurological pathway

Sl. No.	Proteins involved in cell differentiation, developmental process	Cholinergic pathway	Neurodegenerative Diseases	Neurotrophin signaling pathway
1.	Neurexophilin-4 (motor function in synapses)	Calcium/calmodulin-dependent protein kinase type II subunit delta (cell plasticity)	Putative solute carrier family 22 member 31 (neuronal dysfunction)	Neurotrophin-4 (Cell differentiation, cell survival and axonal out growth)
2.	Neural cell adhesion molecule 2 (cell-cell adhesion, neuronal out growth, axonal plasticity)	Calcium/calmodulin -dependent protein kinase type II subunit delta (cell plasticity)	Tubulin alpha-8 chain (axonal transport defects)	Calcium/calmodulin -dependent protein kinase type II subunit delta (cell plasticity)
3.	Nyctalopin (Retinal cell synapse protein)	Voltage-dependent L-type calcium channel subunit alpha-1C	Low-density lipo protein receptor-related protein 6 (axonal transport defects)	Pigment epithelium-derived factor (Cellular developmental process, wound healing)
4.	Treacle protein (Developmental process)	Adenylate cyclase type 6	Glutamate receptor ionotropic, delta-1	----
5.	Ras-related protein Rab-30 (vesicle transport)	----	Spectrin beta chain, non-erythrocytic 1	----
6.	Growth/differentiation factor 9 (growth and differentiation)	---	Dynactin subunit 1 (axonal transport defects)	---
7.	Syntaxin-binding protein 5 (vesicle trafficking and exocytosis inhibition)	---	Voltage-dependent L-type calcium channel subunit alpha-1C	---

Discussion

Demyelination is a challenging clinical condition demanding novel approaches. In this study, the role of BM-MSCs and its CM on restoring myelination was evaluated in vivo in demyelinated rat model established PSNL.

The study demonstrated successful restoration of myelination using both BM-MSCs and CM with BM-MSC having better effect suggested by both histological and ultrastructural anlaysis. The evaluation of CM revealed many proteins and growth factors secreted by the MSCs involved in various functional annotations like biological process, cellular component involvement, molecular function processes etc. mentioned later in the discussion.

Although report on role of MSCs in nerve regeneration and repair were present, however, there were no evidence to prove the beneficial effect of MSCs to be via transdifferentiation into functional neural cells at the injury site of the PNS. Apart from properties such as repair, regeneration, immunoregulatory aspect etc. yet another emerging aspect of MSCs gaining attention is its paracrine effects reported in preclinical studies[15, 16]. Previous studies in CNS urged us to investigate both cell-based and cell free approach in restoring myelination in this study[17, 18].

In this study, we generated a surgically induced demyelinated rat model using PSNL by modified protocol developed by Seltzer,1990. PSNL caused demyelination in the sciatic nerve was in coherence with reports from other groups[19].

Histological studies revealed distorted architecture in the DEM nerves as compared to control however, improved overall architecture was observed in both BM-MSC and CM treated group[20]. Nevertheless, self-recovery group also displayed signs of improvement as compared to DEM group.

Immunostaining revealed reduced MBP expression and fiber loss suggesting demyelination further confirmed by semiquantitative analysis for MBP expression. Both BM-MSC and CM treatment significantly increased MBP expression, confirmed by semiquantitative analysis for MBP positive cells, with more effect in BM-MSC group. In self-recovery group, significant increase in expression of MBP was observed as compared to DEM group, however effect was lesser than intervention groups.

Histochemical staining (Kpal) for myelin further confirmed the above findings with decreased myelin intensity in DEM and upon treatment intense myelin rings observed along with thinly populated myelin rings suggesting remyelination.

Furthermore, ultrastructural examination revealed disrupted myelin sheath, interaxonal gaps and axonal shrinkage in the DEM group. Morphometric analysis reported reduced myelin thickness, axonal radius and increased g ratio in DEM group. Upon intervention, reduced axonal shrinkage, interaxonal gaps and improved myelin thickness were observed in BM-MSC treated group validated further by morphometric analysis with significant increase in

axonal radius and myelin thickness and decreasing g ratio towards optimal PNS value (~0.6). Our results were in similar line with other studies reported[21-24]. Although CM treated group displayed partial improvement no significant difference was depicted by morphometric analysis.

Although most of the effects of BM-MSCs reported are via paracrine secretions[9, 25, 26]. However, in our study we observed better response in BM-MSC treated group as compared to CM. Our findings were in similar lines with another group suggesting restoration in MSCs treated groups to be more than the CM injected group[27]. To the best of our knowledge, our group has reported for the first time the effect of BM-MSCs and the CM on myelin restoration reporting extensive histological and morphometric evaluation of myelin.

Culminating these evidences, we speculated that analysis of the secretome might identify the paracrine factors enabling the development of cell-free therapies mimicking their effects in various demyelinating conditions. Secreted proteins such as Tubulin alpha-8 chain, Spectrin β chain, Neurexophilin-4, NCAM2 etc. were involved in neurological pathways. Additionally, these secreted proteins were found to be involved in various structural and functional annotations like biological and molecular function processes, cellular component involvement, developmental process, multicellular organ development, extracellular matrix structure etc. as per the STRING data analysis. However, proteins associated in myelination and neurotrophic factors were not much evident possibly be due to variations in cultures dependent on subject donor, tissue source and culture conditions[28, 29]. Nevertheless, it is noteworthy that secretome composition can be induced based upon preconditioning them to improve specific profiles apt for the injured tissue[30]. This could have led to the lesser effect of CM observed in our study as compared to the cells. We speculate, that the whole cell proteome analysis of BM-MSCs may give any clue for the presence of myelinated proteins since nothing has been reported yet.

The limitation of this study is lack of electrophysiological studies to confirm functional restoration. Further studies including functional assays could augment the findings.

To conclude the study demonstrates successful remyelination using both BM-MSCs and CM, more so by cell-based therapy. The evidence of various growth factors in the secretome of BMSC is a promising finding which could pave way for clinical applications.

Materials and Methods

Ethics approval/ Ethics Statement

For the usage of human samples (BM-MSCs), the experimental protocol was approved by Institutional Ethics Committee (Ref. No. UH/IEC/2020/245) and Institutional Committee for Stem Cell Research (Ref. No. UH/ICSCR/2022/2) at University of Hyderabad, Hyderabad, India. Informed consent was obtained from all subjects and/or their legal guardian(s) from the previous approved project from our lab. All experiments were performed in accordance with relevant guidelines, regulations and in line with the principles of the Declaration of Helsinki.

For in vivo work involving animals, the experimental protocol was approved by Institutional Animal Ethics Committee (IAEC) (Ref. No. UH/IAEC/GVK/2023-1/01), University of Hyderabad, Hyderabad, India. All the methods were performed in accordance with the relevant guidelines and regulations- "ARRIVE- (Animal Research: Reporting of *In Vivo* Experiments)" and IAEC, University of Hyderabad guidelines. Anaesthesia and euthanasia were executed as per the guidelines of IAEC, University of Hyderabad and American Veterinary Medical Association (AVMA) Guidelines for the Euthanasia of Animals (2020).

Animals

Male Sprague Dawley (SD) rats (200-250g) were purchased from Vyas Labs, Amberpet, Hyderabad, India. Animals were housed in standard 25±1°C housing condition and 12h light:12h dark at animal house facility, University of Hyderabad, Hyderabad, India during the study and were given access to feed and water ad libitum. The animals were acclimatized for one week before study inception. guidelines. At the end of the experiment the animals were euthanized using Co_2 asphyxiation and sciatic nerve were harvested for performing various histopathological and ultrastructural studies.

Experimental groups

The animals were divided into 4 groups explained in Table 1. All the groups underwent surgical intervention excluding Control group. Control and Self-recovery group were administered sterile PBS during the intervention while remyelination group were administered cells (BM-MSCs) and conditioned media (CM) respectively. DEM group underwent partial sciatic nerve ligation (PSNL) and was euthanized after 3 weeks post-surgery for validating demyelination. Rest all groups were euthanized after 6 weeks from the day of inception of the study. The DEM group was euthanized using Co_2 asphyxiation on 21st day, sciatic nerve harvested and stored in 10%

formalin (H&E, IHC) and 2.5% glutaraldehyde (Kpal staining and TEM). Demyelination was evaluated on 21st day by histopathology, immunohistochemistry (MBP), myelin staining (Kpal) and TEM. Rest all groups were maintained under standard experiments until the termination of the study.

Table 1. Representation of number of animals, animal groups and interventions used in the study

Animal Groups	**Surgical Intervention**	**Therapeutic Intervention**	**No. of animals /group**
Group-I: Control	No	Sterile PBS	N=6
Group-II: Demyelination (DEM)	Partial Sciatic Nerve Ligation (PSNL)	No	N=6
Group-III: Self-recovery	Partial Sciatic Nerve Ligation (PSNL)	Sterile PBS	N=6
Group-IV: Remyelination (REM)	Partial Sciatic Nerve Ligation (PSNL)	a. Cells (BM-MSC) b. Conditioned Media (CM)	N=6

Generation of demyelinated animal model using partial sciatic nerve ligation (PSNL)

Healthy male Sprague Dawley (SD) rats weighing 250g were used for the study. SD rats were anesthetized using combination of Ketamine (90mg/kg)/Xylazine(10mg/kg) (i.p.). Demyelination was induced using PSNL described by Seltzer. Briefly, to induce injury (demyelination), the sciatic nerve was partially ligated to 1/3rd of the diameter using 6-0 monofilament sutures. Control groups were left untouched. Anti-inflammatory and antibiotic were administered twice daily for 5 days for healthy recovery of the animals. Demyelination was validated by histochemistry, immunohistochemistry and electron microscopy.

Validation of demyelination and remyelination

Haematoxylin and Eosin staining

The paraformaldehyde-fixed tissues were dehydrated and embedded in paraffin. The tissues were sectioned transversely at 4µm. The tissue cross-sections were deparaffinized twice in xylene, and then rehydrated twice, for 3 min each, in graded alcohol 100%, 95%, 80%, and 70% and washed under tap water for 10 minutes. The slides

were dipped in hematoxylin for 3 minutes, followed by eosin staining for 2 minutes followed by washing under tap water for 6 minutes. Sections were rehydrated by being exposed to graded alcohol 70%, 95% and 100% followed by two xylene washes. The slides were mounted and images were captured using image scanner (Optimum 6X, Morphle machine).

Histochemistry for Myelin staining

The fixed nerve tissue was incubated in Kpal stain (1% Chromic acid, 1% Osmium tetroxide and 2 drops Glacial acetic acid) for 24 h followed by dehydration and paraffin embedding. Tissues were sectioned transversely at 4µm followed by deparaffinization and rehydration. The slides were incubated in a mixture of Hematoxylin, propanol and water solution for 30 minutes in hot air oven at 95°C followed by dipping in 0.5% KMN04.Ths slide was dipped in 1% Oxalic acid for 30 seconds followed by washing in water. The counterstaining was done with eosin followed by alcohol dip if required. The slides were mounted and images were captured using image scanner (Optimum 6X, Morphle machine).

Immunohistochemistry for Myelin Basic Protein

The tissues were fixed in 10% buffered formalin and 4µm thin sections were prepared from paraffin embedded tissue blocks. The tissue sections were heated at 70°C for 15 minutes for de-paraffinization. These sections were dipped in xylene thrice for 5 minutes each and rehydration was performed by dipping in 100%, 90%, and 80% alcohol, respectively, for 5 minutes. Slides were rinsed in running tap water for 1 minute. Antigen retrieval was performed by heating the slides in citrate buffer (pH = 6) thrice for 5 minutes each in a microwave. The slides were allowed to cool down to RT followed by blocking in 2.5% BSA for 45 mins at RT. Tissue sections were stained using MBP (1:200, MAB42282, Thermofischer) overnight at 4°C. The slides were incubated with Poly-HRP conjugated secondary antibody (1:1000) followed by addition of DAB substrate. Counterstaining was done in hematoxylin. All the above steps were followed by PBS washes. The slides were visualized using and images were captured using (Optimum 6X, Morphle machine).

Ultrastructural and morphometric evaluation by electron microscopy

TEM studies were performed at Ruska Labs, Agriculture University, Hyderabad. Briefly, the nerve tissue was fixed in 2.5% glutaraldehyde in phosphate buffer (0.1M, pH 7.2) at 4°C overnight. The tissues were washed with PBS, and post-fixed in 1% osmium tetroxide for 3h. Fixed specimens were washed, dehydrated, infiltrated and embedded in Araldite resin. Ultrathin sections (50-70 nm) were made using ultra-microtome (Leica Ultra cut UCT-GA-D/E-1/100), mounted on copper grids and stained with uranyl acetate and Reynolds lead citrate.

Sections were scanned using Transmission Electron Microscope (JEM 1400 Flash, JEOL India Pvt. Ltd.) in NIAB, Hyderabad.

Restoration of myelination using BM-MSC and conditioned media

Isolation and establishment of BM-MSC cultures

Human BM-MSCs were harvested by modification of previously published protocol[31-33]. Briefly, the bone marrow mononuclear cells were harvested by centrifugation using Histopaque®-1077(10771, Sigma Aldrich, USA). Hravested mononuclear cells were resuspended in Dulbecco's Modified Eagle's Medium (1190565, Thermo Fisher, USA) supplemented with 10% FBS (fetal bovine serum;Gibco), antibiotic-antimycotic (15240096, Gibco^{TM}) and plated at seeding density of 1x10^6 cells/ml in T75 flasks (Corning). Non-adherent cells were discarded after 48h, with fresh media replaced every 2-3 days to the adherent cells, maintained at 37℃, 5% CO_2. Once 80% confluent, they were passaged using TryplE (12604013, Thermo Fisher USA). Harvested cells confirmed the ISCT criteria for MSCs i.e. plastic adherence, CD105, CD73, CD90 positive and CD34, CD45 and HLA-DR negative and differentiation into mesodermal lineage[33].

Harvesting MSC-CM

BM-MSCs from P_3 generation were used for harvesting CM. Once 80-90% confluent, the cells were cultured in serum free media (DMEM; Invitrogen; high glucose 4.5 mg/L without FBS) for 48h. Post 48 h, the CM was collected and dead cells were removed by centrifugation. The medium was further concentrated using 3KDa amicon filters and the concentrate stored at -80°C until further use.

Intravenous transplantation of MSCs (cells) and CM

At 80% confluency, the cells were trypsinized using TrypLE (12604013, Thermo Fisher USA) counted and suspended in PBS. CM stored at -80℃ was used for therapeutic intervention. At 21st day post-surgery, 100µl of BM-MSCs (1x10^6 cells/100µl) and 100µl CM was intravenously injected/animal in BM-MSC and CM group respectively. Control and self-recovery groups were injected 100µl of sterile culture grade PBS i.v.

Recovery of myelination induced by transplantation of BM-MSC and CM

The treatment groups were euthanized after 6 weeks. Harvested tissue was collected in 10% formalin/2.5% glutaraldehyde based on the experiments. The tissues were processed as per the experimental protocol and evaluated for remyelination by H&E staining, histochemistry for myelin staining, immunohistochemistry and morphometric evaluation as mentioned above.

Sample preparation and characterization of the conditioned media for MS analysis

BM-MSCs were cultured in DMEM supplemented with 10% FBS till 80-85% confluency. For collecting CM, cells were incubated in serum free media for 12-24 h to eliminate any serum derived contaminants like serum albumin. CM was concentrated to 0.2 to 0.5 ml using 3Kda cutoff filters and protein concentration was estimated using Bradford method. Sample preparation was done by trypsin digestion and 100-250 µg protein was used for mass spectrometry analysis. The proteins were reduced (DTT), alkylated (Iodoacetamide) and digested using trypsin (sequencing grade) digestion (20:1) for 12-16 h. Digestion was terminated by adding 0.1 % formic acid. The peptides were isolated in 0.1% formic acid, desalted using zip tips concentrated using speed vac. Samples were analyzed using Thermo Scientific Orbitrap Q Exactive HF with Ultimate 3000 nano LC mass spectrometer system with 180 minutes total run time using gradient buffer system (Solvent A-water with 0.1% Formic Acid, Solvent B-80% Acetonitrile with 0.1% Formic Acid with 0.2 µl/min with positive polarity, and +2 default charge state. The peptides were analyzed using Proteome Discoverer 2.4 software and identified proteins analyzed using STRING DATABASE and DAVID annotation tool for functional analysis.

Statistical Analysis

All results are expressed as mean value ± standard error mean (SEM) from three independent experiments. Statistical analysis was done using GraphPad Prism 8 (GraphPad Software, San Diego, CA, USA) using one way analysis of variance (ANOVA) for comparing three or more groups, value of $p < 0.05$ was considered to be statistically significant whereas $P > 0.05$ meant nonsignificant and are represented as "ns."

Declarations

Acknowledgements

The authors would like to acknowledge Dr. Tarun; Veterinarian, UoH Animal house facility, Preethi Prasanna; NIAB, Maheshwari, Deepa and Ramya; NIMS for helping in the study.

Source of funding

The authors thank the Indian Council of Medical Research, for Senior Research Fellowship to Aparna Mohanty (2021-12098/SCR-BMS) and IoE, DST PURSE, UPE-II, ICMR grant (2021-14627/SCR/Adhoc-BMC) for financial support.

Author's contribution

GKV: Supervision, Conceptualization, Formal analysis and investigation, Writing- reviewing and editing, Funding acquisition, Resources. AM and AVS: Methodology, Data collection, Formal analysis and investigation,

Writing- original draft preparation, reviewing and editing. MU: Formal analysis and investigation, Writing- reviewing and editing

Conflict of interest

The authors declare that they have no competing interests.

Data availability statement

All data generated or analysed during this study are included in this published article.

References

1. Martyn, C.N. and R.A. Hughes, *Epidemiology of peripheral neuropathy.* J Neurol Neurosurg Psychiatry, 1997. **62**(4): p. 310-8.doi:10.1136/jnnp.62.4.310
2. Kornfeld, T., P.M. Vogt, and C. Radtke, *Nerve grafting for peripheral nerve injuries with extended defect sizes.* Wien Med Wochenschr, 2019. **169**(9-10): p. 240-251.doi:10.1007/s10354-018-0675-6
3. De la Rosa, M.B., E.M. Kozik, and D.S. Sakaguchi, *Adult Stem Cell-Based Strategies for Peripheral Nerve Regeneration.* Adv Exp Med Biol, 2018. **1119**: p. 41-71.doi:10.1007/5584_2018_254
4. Piovesana, R., et al., *Schwann-like adipose-derived stem cells as a promising therapeutic tool for peripheral nerve regeneration: effects of cholinergic stimulation.* 2021. **16**(6): p. 1218-1220.doi:10.4103/1673-5374.300433
5. Levi, A.D., et al., *The Use of Autologous Schwann Cells to Supplement Sciatic Nerve Repair With a Large Gap: First in Human Experience.* Cell Transplant, 2016. **25**(7): p. 1395-403.doi:10.3727/096368915X690198
6. McGrath, A.M., et al., *Fibrin conduit supplemented with human mesenchymal stem cells and immunosuppressive treatment enhances regeneration after peripheral nerve injury.* Neurosci Lett, 2012. **516**(2): p. 171-6.doi:10.1016/j.neulet.2012.03.041
7. Yousefi, F., et al., *Novel approaches using mesenchymal stem cells for curing peripheral nerve injuries.* Life Sci, 2019. **221**: p. 99-108.doi:10.1016/j.lfs.2019.01.052
8. Kubiak, C.A., et al., *Stem-cell-based therapies to enhance peripheral nerve regeneration.* Muscle Nerve, 2020. **61**(4): p. 449-459.doi:10.1002/mus.26760
9. Namini, M.S., et al., *Cell-free therapy based on extracellular vesicles: a promising therapeutic strategy for peripheral nerve injury.* Stem Cell Res Ther, 2023. **14**(1): p. 254.doi:10.1186/s13287-023-03467-5
10. Sivanarayanan, T.B., et al., *Allogenic bone marrow-derived mesenchymal stem cells and its conditioned media for repairing acute and sub-acute peripheral nerve injuries in a rabbit model.* Tissue and Cell, 2023. **82**: p. 102053.doi:https://doi.org/10.1016/j.tice.2023.102053
11. Burdon, T.J., et al., *Bone marrow stem cell derived paracrine factors for regenerative medicine: current perspectives and therapeutic potential.* Bone Marrow Res, 2011. **2011**: p. 207326.doi:10.1155/2011/207326
12. Kanehisa, M., *Toward understanding the origin and evolution of cellular organisms.* Protein Sci, 2019. **28**(11): p. 1947-1951.doi:10.1002/pro.3715
13. Kanehisa, M., et al., *KEGG: biological systems database as a model of the real world.* Nucleic Acids Res, 2025. **53**(D1): p. D672-d677.doi:10.1093/nar/gkae909
14. Kanehisa, M. and S. Goto, *KEGG: kyoto encyclopedia of genes and genomes.* Nucleic Acids Res, 2000. **28**(1): p. 27-30.doi:10.1093/nar/28.1.27
15. Chopp, M. and Y. Li, *Treatment of neural injury with marrow stromal cells.* Lancet Neurol, 2002. **1**(2): p. 92-100.doi:10.1016/s1474-4422(02)00040-6
16. Neuhuber, B., et al., *Axon growth and recovery of function supported by human bone marrow stromal cells in the injured spinal cord exhibit donor variations.* Brain Res, 2005. **1035**(1): p. 73-85.doi:10.1016/j.brainres.2004.11.055
17. Lee, J.S., et al., *A long-term follow-up study of intravenous autologous mesenchymal stem cell transplantation in patients with ischemic stroke.* Stem Cells, 2010. **28**(6): p. 1099-106.doi:10.1002/stem.430

18. Crigler, L., et al., *Human mesenchymal stem cell subpopulations express a variety of neuro-regulatory molecules and promote neuronal cell survival and neuritogenesis.* Exp Neurol, 2006. **198**(1): p. 54-64.doi:10.1016/j.expneurol.2005.10.029
19. Seltzer, Z., R. Dubner, and Y. Shir, *A novel behavioral model of neuropathic pain disorders produced in rats by partial sciatic nerve injury.* Pain, 1990. **43**(2): p. 205-218.doi:10.1016/0304-3959(90)91074-s
20. Lei, C., H. Chen, and K. Chen, *Effects of Bone Marrow Mesenchymal Stem Cells on Myelin Repair and Emotional Changes of a Cuprizone-Induced Demyelination Model.* J Integr Neurosci, 2023. **22**(2): p. 40.doi:10.31083/j.jin2202040
21. Galhom, R.A., H.H. Hussein Abd El Raouf, and M.H. Mohammed Ali, *Role of bone marrow derived mesenchymal stromal cells and Schwann-like cells transplantation on spinal cord injury in adult male albino rats.* Biomed Pharmacother, 2018. **108**: p. 1365-1375.doi:10.1016/j.biopha.2018.09.131
22. Chomiak, T. and B. Hu, *What is the optimal value of the g-ratio for myelinated fibers in the rat CNS? A theoretical approach.* PLoS One, 2009. **4**(11): p. e7754.doi:10.1371/journal.pone.0007754
23. Han, J.W., et al., *Bone Marrow-Derived Mesenchymal Stem Cells Improve Diabetic Neuropathy by Direct Modulation of Both Angiogenesis and Myelination in Peripheral Nerves.* 2016. **25**(2): p. 313-326.doi:10.3727/096368915x688209
24. Rushton, W.A., *A theory of the effects of fibre size in medullated nerve.* J Physiol, 1951. **115**(1): p. 101-22.doi:10.1113/jphysiol.1951.sp004655
25. Raoofi, A., et al., *Bone Marrow Mesenchymal Stem Cell Condition Medium Loaded on PCL Nanofibrous Scaffold Promoted Nerve Regeneration After Sciatic Nerve Transection in Male Rats.* Neurotox Res, 2021. **39**(5): p. 1470-1486.doi:10.1007/s12640-021-00391-5
26. Chen, Y.T., et al., *The superiority of conditioned medium derived from rapidly expanded mesenchymal stem cells for neural repair.* Stem Cell Res Ther, 2019. **10**(1): p. 390.doi:10.1186/s13287-019-1491-7
27. Tahmasebi, F., et al., *The comparative effects of bone marrow mesenchymal stem cells and supernatant transplantation on demyelination and inflammation in cuprizone model.* Mol Biol Rep, 2024. **51**(1): p. 674.doi:10.1007/s11033-024-09628-w
28. Contreras, E., et al., *New insights into peripheral nerve regeneration: The role of secretomes.* Experimental Neurology, 2022. **354**: p. 114069.doi:https://doi.org/10.1016/j.expneurol.2022.114069
29. Rizk, M., et al., *Heterogeneity in Studies of Mesenchymal Stromal Cells to Treat or Prevent Graft-versus-Host Disease: A Scoping Review of the Evidence.* Biology of Blood and Marrow Transplantation, 2016. **22**(8): p. 1416-1423.doi:https://doi.org/10.1016/j.bbmt.2016.04.010
30. Ferreira, J.R., et al., *Mesenchymal Stromal Cell Secretome: Influencing Therapeutic Potential by Cellular Pre-conditioning.* 2018. **Volume 9 - 2018**.doi:10.3389/fimmu.2018.02837
31. Koppula, R.P., N. Polisetti, and G.K. Vemuganti, *Unstimulated diagnostic marrow tap – a minimally invasive and reliable source for mesenchymal stem cells.* 2010. **34**(3): p. 275-281.doi:https://doi.org/10.1042/CBI20090142
32. Polisetti, N., et al., *Isolation, characterization and differentiation potential of rat bone marrow stromal cells.* Neurol India, 2010. **58**(2): p. 201-8.doi:10.4103/0028-3886.63789
33. Jaffet, J., et al., *Human Lacrimal Gland Derived Mesenchymal Stem Cells - Isolation, Propagation, and Characterization.* Invest Ophthalmol Vis Sci, 2023. **64**(10): p. 12.doi:10.1167/iovs.64.10.12

Tables

Table 1. Representation of number of animals, animal groups and interventions used in the study

Table 2: KEGG pathway analysis of BM-MSC secretome proteins involved in neurological pathway

Legends

Fig.1 Histological and morphometric validation of surgically induced demyelination in sciatic nerve. Representative images of sections of sciatic nerve processed for H&E staining in different groups. a) Control b) DEM. Representative images of Myelin (Kpal) stain on sciatic nerve sections of various groups c) Control d) DEM. Immunohistochemistry (IHC) images for myelin basic protein (MBP) e) Control f) (DEM) g) Semi

quantitative analysis of IHC showing MBP positive cells in different groups. Representative images of ultrastructural examination of sciatic nerve sections in different groups h, i, j) Control k, l, m (DEM). Quantification of various parameters from morphometric analysis of sciatic nerve sections in different groups n) g ratio (p***<0.01) Control vs DEM o) myelin thickness. (p****<0.0001) Control vs DEM p) axon radius. (p***<0.001) Control vs DEM. Scale bar for TEM micrographs h, i, k) 1µm, l) 500nm j, m)200nm. Scale bar 500µm and insert scale bar 20µm for H&E images. Scale bar 200µm and insert scale bar 20µm for myelin staining and IHC images. Data reported as mean ± standard deviation. p***<0.001 compared to control for IHC quantification).

Fig.2 Histological and morphometric evaluation of remyelination post interventions. Representative images of sections of sciatic nerve processed for H&E staining in different groups. a) Control b) DEM c) Self-recovery d) BM-MSC e) CM. Myelin (Kpal) stain on sciatic nerve sections of various groups f) Control g) DEM h) Self-recovery i) BM-MSC j) CM. Immunohistochemistry (IHC) images for myelin basic protein (MBP) k) Control l) DEM m) Self-recovery n) BM-MSC o) CM p) Semi quantitative analysis of IHC showing MBP positive cells in different groups. Image scale bar 500µm and insert scale bar 20µm for H&E images. Image scale bar 200µm and insert scale bar 20µm for myelin staining and IHC images. Data reported as mean ± standard deviation. p***<0.001 compared to control, p#<0.01, p##<0.001 and p###<0.001 compared to demyelinated (DEM) group.

Fig.3 Representative images of ultrastructural examination of sciatic nerve sections in different groups. a, b, c) control d, e, f) DEM g, h, i) self-recovery j, k, l) BM-MSC m, n, o) Cells. # represents schwann cell nucleus, blue arrow represents degenerating myelin, orange triangle represents intact myelin, red star represents intact axon, yellow arrow represents inter axonal gap and axonal shrinkage. Scale bar a, d, g, h, m) 500nm, b, e, h, k, n) 1µm, c, f, i, l, o) 200nm. Quantification of various parameters from morphometric analysis of sciatic nerve sections in different groups q) g ratio (p***<0.01) Control vs DEM, (P #<0.01) DEM vs CM, ns=non-significant (p=0.9683) DEM vs CM r) Quantification myelin thickness. (p****<0.0001) Control vs DEM, (p ## <0.001) DEM vs BM-MSCs, ns=non-significant (p=0.9936) DEM vs CM s) axon radius. (p***<0.001) Control vs DEM, (p ###<0.001) DEM vs BM-MSCs, ns=non-significant (p=0.3718) DEM vs CM.

Fig.4 Characterization of secretome by mass spectrometry a) Biological process of BMSC secretome proteins. b) Molecular Function of BMSC secretome proteins c) Cellular proteins of BMSC secretome proteins. The proteins were categorized based on their False discovery rate (FDR) ≤ 0.05 when compared with the whole gene count. X-axis indicates the signal /gene count and the Y-axis indicates the Groups at similarity was set at 0.8.d) Representative image of the interacting proteins in BM-MSC secretome. A typical BM-MSC secretome protein

association network using STRING. The network has been expanded by 346 valid proteins and the confidence cutoff for showing interaction links has been set to “highest” (0.900). The secretome proteins identified showed as various colored nodes. Each node represents all the proteins produced by a single protein-coded gene locus. The interaction of protein with other showed with edges. The line thickness indicates the strength of data support. The interactions of each protein are specific[12-14].